Constructing the Universe with Clusters of Galaxies, IAP 2000 meeting, Paris (France) July 2000
Florence Durret & Daniel Gerbal eds.

Cluster of Galaxies as Gravitational Lenses

Jean-Paul KNEIB

Laboratoire d'Astrophysique, UMR 5572, Observatoire Midi-Pyrénées
14 avenue E. Belin, 31400 Toulouse, France

What is the total mass distribution of a galaxy cluster? What is its mass distribution profile and how does it compares to the numerical simulation predictions? What is the physical/dynamical state of this cluster? How does the lensing mass estimate compares to X-ray/dynamical/SZ estimates? How massive and how extended are cluster galaxies halos? How massive are filaments between cluster of galaxies? What is the gravitational amplification factor of this lensed galaxy? Any redshift estimates for that multiple images and this arclet? What is the lensing corrected number counts for this galaxy population? and the reconstructed morphology of this lensed galaxy? What are the cosmological constraints that can be derived from cluster lenses observations?

This is a non exhaustive list of questions that can be addressed when using gravitational lensing in clusters of galaxies. I will review here lensing in clusters as a *unique* and useful tool in modern *observational* cosmology.

1 Introduction

Cluster of galaxies are the largest and most massive bounded structures in the Universe. Understanding their number distribution and mass distribution is the best way to relate observation to theoretical expectations and simulations. Due to their large mass density galaxy clusters (as well as galaxies) locally deform the Space-Time (see Fig. 1). Therefore, the wave front of any light coming from a distant source passing through a galaxy cluster will be distorted. Moreover, for the most massive clusters the mass density in the core is high enough to break the wave front comming from a distant source into pieces hence producing multiple images, which then usually form these extraordinary gravitational giant arcs (the *strong lensing* domain). Distant optical/NIR galaxies will thus appeared distorted and magnified, we usually call them arclets because of their noticeable elongated shape tangentially aligned toward the cluster center. Note however that their shape is a combination of the intrinsic shape and the distortion induced by the cluster. If the alignment between the observer, the cluster and distant galaxies is less perfect the distortion induced by the cluster will be less important and can not be recognize immediately – statistical method are required – (the *weak regime* domain). Indeed in this region, the

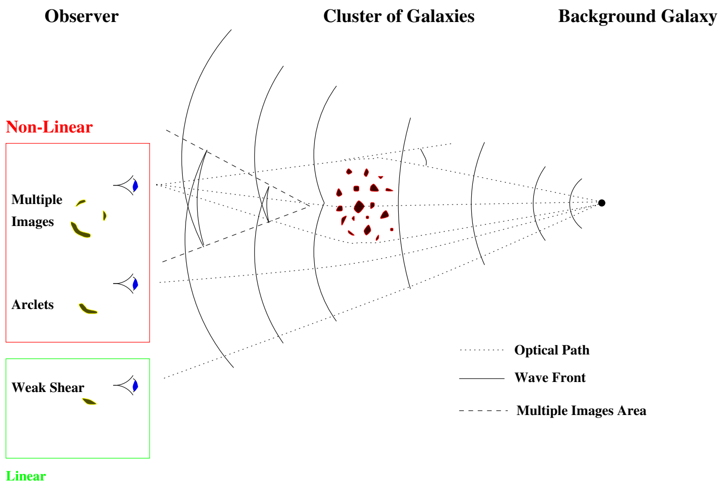

Figure 1: Gravitational lensing in clusters: A simple representation of how gravitational images are formed.

shape of the galaxies are dominated by their intrinsic ellipticity or worse contaminated by the distortion of the camera and/or the point spread function (PSF) of the image.

In the thin lens approximation (which usually holds for cluster-lenses *e.g* Schneider, Ehlers & Falco, 1992), the deflection of light between the position of the source $\vec{\theta}_S$ and the position of the image $\vec{\theta}_I$ is given by the lensing mapping equation:

$$\vec{\theta}_S = \vec{\theta}_I - \frac{2\mathcal{D}}{c^2}\vec{\nabla}\phi_N^{2D}(\vec{\theta}_I) = \vec{\theta}_I - \vec{\nabla}\varphi(\vec{\theta}_I) \quad (1)$$

where $\mathcal{D} = D_{LS}/D_{OS}$ is the angular distance ratio between the Lens and the Source and the Observer and the Source [this ratio therefore depends on the redshift of the cluster z_L and the background source z_S, as well as - but only weakly - on the cosmological parameter Ω_m and Ω_λ], ϕ_N^{2D} is the Newtonian projected gravitational potential, and φ the lensing potential. This transformation is thus a mapping from Source plane to Image plane, and the Hessian of this transformation (also called the magnification matrix) relates a source element of the Image to the Source plane:

$$\frac{d\vec{\theta}_S}{d\vec{\theta}_I} = \mathcal{H} = \mathcal{A}^{-1} = \begin{pmatrix} 1-\partial_{xx}\varphi & -\partial_{xy}\varphi \\ -\partial_{xy}\varphi & 1-\partial_{yy}\varphi \end{pmatrix} = \begin{pmatrix} 1-\kappa-\gamma_1 & -\gamma_2 \\ -\gamma_2 & 1-\kappa+\gamma_1 \end{pmatrix} \quad (2)$$

where we have defined the convergence $\kappa = \Sigma/2\Sigma_{crit}$, the shear $\vec{\gamma} = (\gamma_1, \gamma_2)$ and the magnification matrix $\mathcal{A}$. This matrix also governs the shape transformation from the Source to the Image plane.

Thus, cluster lenses can be used in 2 ways: *i)* Firstly by understanding and modeling the gravitational optics of this system: by probing the **total mass** distribution of the cluster – which explains the observed image configuration and distortions –, by constraining the **distance** of the lensed galaxies – the more distant the more distorted they are –, to put constraints on the cosmological parameters - although this is a second order effect –. *ii)* Secondly as a *Natural telescope*: galaxies seen through massive cluster cores are amplified by the gravitational lensing effect making them easier to study in details; the faintest/unresolved sources – which would otherwise remain unknown – can be detected/identified, and the brighter/resolved sources can be studied in detailed either specrtoscopically or morphologically.

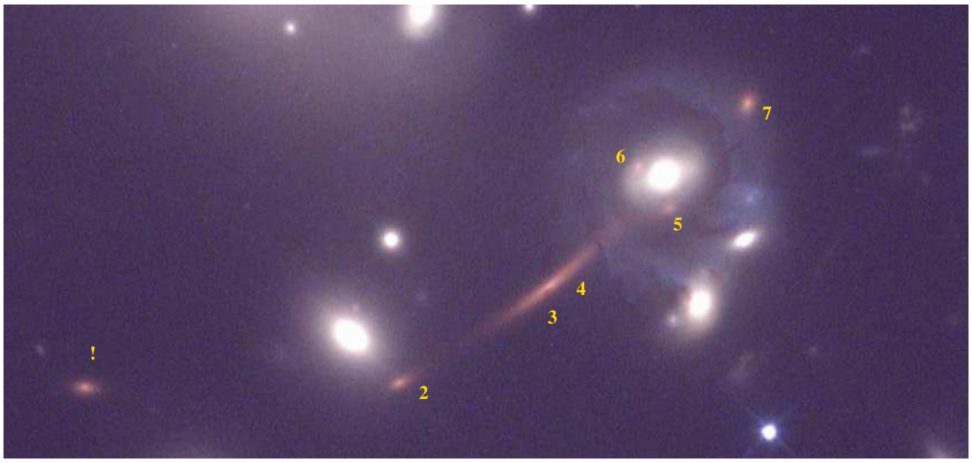

Figure 2: A spectacular case of multiple images in the cluster Abell 2218 seen in the BRI HST image. The distant E/S0 galaxy at z=0.702 is lensed into a 7-image configuration.

2 Cluster Lens Properties

2.1 Strong Lensing

Massive clusters can produce multiple images, this will happen when the surface mass density of the cluster core reach or is larger than the *critical density*: $\Sigma_{crit} = \frac{c^2}{4G}\frac{D_{OS}D_{OL}}{D_{LS}}$. The configuration of multiple images tells us about the structure of the mass distribution. A cluster with one dominant clump of mass will produce *fold* or *cusp* arcs, radial arcs (*e.g* MS2137.3-2353: Fort et al. 1992, Mellier et al. 1993; AC114: Natarajan et al. 1998; A383: Smith et al. 2000); a bimodal cluster can produce straight arcs (*e.g* Cl2236-04: Kneib et al. 1994a), triplets (A370: Kneib et al 1993, Bezecourt et al. 1999) or even triangular image; a very complex structure with lots of massive halos in the core can produce multiple image system with 7 or more images of the same source (*e.g* Cl2244-04, A2218 – Fig. 2 –).

A particular useful and popular mass estimate in the strong lensing regime is the mass within the Einstein radius R_E: $M(< R_E) = \pi\Sigma_{crit}\theta_E^2$; R_E is the location of the critical line for a circular mass distribution, usually approximated by the arc radius R_{arc}. It is a very handy expression – independent of the mass profile for a circular mass symmetry –, but one should be careful in using it: either because the arc used to derive the mass as a unknown redshift, or the arc is a single image and thus does not trace the Einstein radius (for a singular isothermal sphere model, a single image can not be closer to twice the Einstein radius or it will have a counter image!), or the mass distribution is very complex with a lot of sub-structure. In conclusion, *this estimator does generally overestimate the mass.*

For galaxy cluster the radial critical line is generally accessible as radial arcs have been discovered in a few cluster lenses now (see Smith et al. 2000 for a recent example). These features are important as they lie very close to the cluster core, and thus provide a *unique* way to probe the mass surface density in the very center. Although none of the observed radial arcs have a spectroscopic measured redshift yet, it seems that they all favors a relatively cuspy mass distribution which is also expected due to the presence of a cD galaxy at the center of the cluster.

The only route to accurately constrain the mass in cluster cores is to use multiple images with a spectroscopic redshift to absolutely calibrate the mass. As the problem is generally degenerate –*in the sense that there is not a single mass distribution but a family of model that is fitting the observables* –, one should used physically motivated representation of the mass distribution and adjust it in order to best reproduce the different family of multiple images (*e.g*

Kneib et al. 1996). As the position of the images are known to great accuracy and are usually located in different places of the cluster cores a simple mass model with one clump can usually not reproduce the image configuration. The lens model needs to include the cluster galaxies to match up the image configuration and positions. As there is not an infinite number of multiple images and thus number of constraints, it is important to limit the number of free parameters of the model and keep it physically motivated – as in the end – we are interested to derive physical properties of the cluster. Alternative method, using non-parametric description have been explored (*e.g.* Abdelsalam et al. 1999), but usually lack the resolution of a parametric form due to the large dynamical range of the mass density expected in a cluster core - but clearly this is an interesting approach than should explored further.

The strong lensing mass modeling technique is an iterative method, in the sense that once a multiple images is securely identified, other multiple images systems can be discovered using morphological/color/redshift-photometric criteria as well as the predictions from the lens model. The lens model can then predict redshift for these multiple systems (Kneib et al. 1993, Natarajan et al. 1998) as well as for the arclets (Kneib et al. 1994b, 1996): on the basis that on average a distant galaxy is randomly orientated, and its ellipticity follow a relatively peaked ellipticity distribution. These prediction can then be tested/verified (*e.g.* Ebbels et al. 1998) and an improved mass model can be derived integrating the new constraints. The ultimate step of strong lensing modeling is to constrain the cosmological parameters that enters in the lensing equations through the D_{LS}/D_{OS} term. This can be undertaken, when in a cluster core, a sufficient number of multiple images (> 3) are identified and for which spectroscopic information can be measured (see Golse et al. this conference).

2.2 Weak Lensing

In the weak lensing regime the game is different: we measure the *mean* ellipticity and/or the *mean* number density of faint galaxies, and we want to relate these statistics to the mean surface mass density κ of the cluster. There are two issues in doing that:

• one for a *theorist*: What is the best method to reconstruct the mass distribution κ (as a mass map or a radial mass profile) from the 'shear field' $\vec{\gamma}$ and/or the magnification bias?

• one for an *observer*: How best determined the 'true' ellipticity of a faint galaxy which is smeared by a PSF barely smaller than the object (when using ground-based images) that is not circular (camera distortion, tracking errors ...) and not stable in time? How best estimate the variation in the number density of faint galaxies due to the lensing effect, taking into account the crowding effect due to the cluster and the intrinsic fluctuations in the distribution of galaxies?

Various approaches have been proposed to solve these two problems, and two families of methods can be distinguished: **direct** and **inverse** methods.

For the theorist issue, the **direct** approaches are: *i)* the Kaiser & Squires (93) method (an integral method, that express κ as the convolution of $\vec{\gamma}$ by a kernel) and subsequent refinements (*e.g.* Seitz et al. 1995, 1996); *ii)* the local inversion method (Kaiser, 1995, Schneider, 1995, Lombardi & Bertin 1998) integrates the gradient of $\vec{\gamma}$ within the boundary of the observed field to then derive κ. The **inverse** approach works on κ or the lensing potential φ and uses maximum likelihood (Bartelman et al. 1996, Schneider et al. 2000) or maximum entropy method (Bridle et al. 1998) to determine the most likely mass distribution (as a 2D mass map or a 1D mass profile) that reproduce the shear field $\vec{\gamma}$ and/or the variation in the faint galaxy number densities. These inverse methods are of great interest as they allow: to quantify the errors in the resultant mass maps or mass estimates (Bridle et al. 2000 – Fig. 3 –), and in principle can cope with external constraints (such as strong lensing, or X-ray) although this has not yet been applied yet to real data.

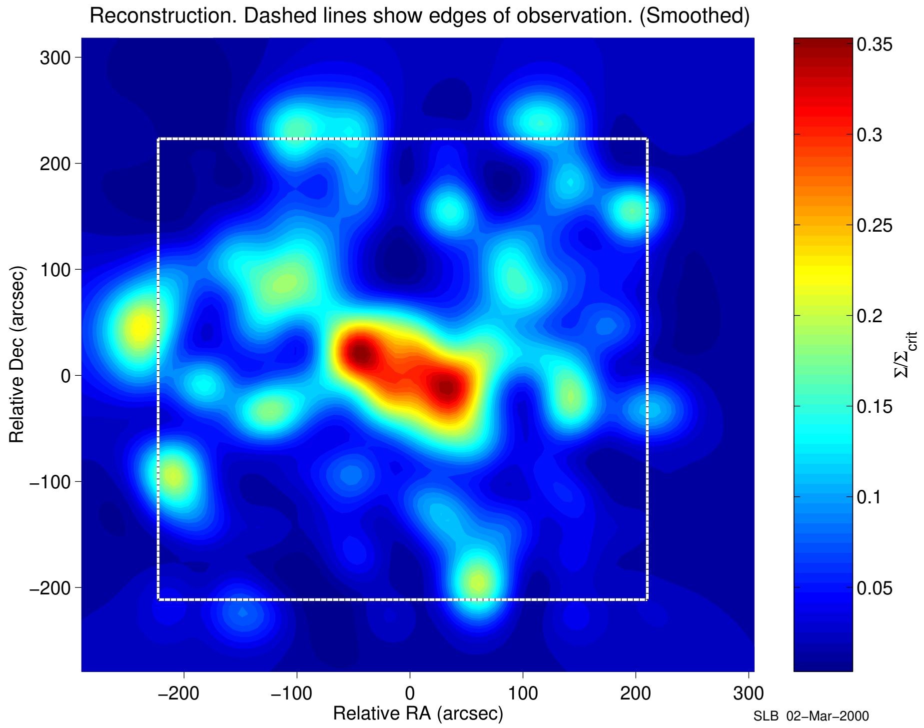

Figure 3: Maximum entropy mass reconstruction (Bridle et al. 2000) of the X-ray luminous MS1054 at $z = 0.83$ using the Clowe Keck dataset (Clowe et al. 2000).

For the observer, before any data handling, the first priority is to choose the telescope that will minimize the source of noise in the determination of the ellipticity of faint galaxies. Although the *Hubble Space Telescope* (*HST*) has the best characteristics in terms of the PSF, it has a very limited field of view not really appropriate to probe the large scale distribution of a cluster (note this is of course less of a problem when looking at high redshift clusters). What is really needed is a wide field imager with excellent PSF and seeing conditions!

Then, we can use a direct approach using for example the Kaiser, Squires and Broadhurst (1995) method [KSB implemented in the *imcat* software], or any other improvement of it (Luppino & Kaiser 1998, Rhodes et al. 2000, Kaiser 2000): that relates the true ellipticity to the observed ellipticity correcting it from the smearing of an elliptical PSF (using the second moments of the galaxy and the PSF).

The inverse approach use maximum likelihood method to find the source galaxy shape that when convolved by the local PSF reproduce best the observed galaxy (*e.g.* Kuijken, 2000). Again the inverse approach has the advantage to give directly an uncertainty in the parameter recovery.

The weak-shear mass reconstruction techniques have been applied to wide-field camera data (UH8k, CFH12k, ESO-WFI, CTIO-MegaCam) and impressive results have started to be published on a high redshift super-cluster (Kaiser et al. 1998) and on low ($z < 0.1$) redshift clusters (Joffre et al. 2000). For high ($z > 0.5$) redshift clusters, large aperture telescope (*e.g.* Clowe et al. 2000) or *HST* (Hoekstra et al. 2000) are probably more adequate.

2.3 Cluster Galaxies Halos

We know that galaxies are massive and that their stellar content does only represent a small part of their total mass. Although the existence of a dark halo has been obvious very early for disk galaxies with the study of their flat velocity curve out to large radius (*e.g.* van Albada et al. 1985), the existence of a dark halo has been accepted for ellipticals only relatively recently (*e.g.* Kochanek 1995, Rix et al. 1997). These studies found that the stellar content dominates the central part of the galaxies, but at distance larger than the effective radius the dark halo dominates the total mass. What is less obvious in cluster of galaxies, is how far the galaxy dark halos extends, as one expect some stripping of the dark halos as they are passing through cluster cores. Furthermore, we would idealy like to relates the strong morphological evolution observed in cluster galaxies (*e.g.* Lewis, Smail & Couch 2000) to their mass properties.

Galaxy lensing effect were first detected in clusters by Kassiola et al (1992) who notes that lengths of the triple arc in Cl0024+1654 can only be explained if the galaxies near the B image were massive enough. Detailed treatment of the galaxy contribution to the cluster mass became important with the refurbishment of the *HST* as first shown by Kneib et al. 1996 – who concluded that galaxies (and their dark halos) in cluster cores contributes by about 10% of the total mass. The theory of what is usually called galaxy-galaxy lensing in clusters was first discussed in details by Natarajan & Kneib 1997, and application to data followed shortly (Natarajan et al. 1998 and Geiger & Schneider 1998). A recent analysis of this effect in various cluster-lenses at various redshift seems to indicate an increase of the cluster ellipticals dark halo size with redshift (Natarajan et al. 2001). Clearly more work is to be done in this direction!

Note, that the standard direct *weak shear* methods generally miss the small scale fluctuations (typically the galaxy halo scales) because of the *averaging* of the galaxy ellipticities. Thus dedicated methods are necessary to probe this effect in the weak shear method. The only easy route is to use an inverse approach which will examine the galaxies **individually**.

2.4 Lensing and other Estimators

Gravitational lensing allow to measure the *total* mass distribution of clusters – and this without making any assumption on the cluster physical state. Other estimators always require some assumption when trying to relate the observables to the *total* mass. Generally these assumptions looks reasonable but may suffer strong bias due to the unknown physical state of the cluster. By providing the *total* mass, lensing does constitute a **key** tool to understand cluster physics. Probably then, the best way is to first derive the total lensing mass using lensing, and then from other observations derive physical properties of the cluster like: dynamical parameters for the galaxy velocities (Natarajan & Kneib 1996), the temperature profile of the X-ray gas (Pierre et al. 1996), the baryon fraction or the equilibrium status of the cluster – however lensing mass estimates have also their limitations (in particular line of sight projection effects).

The alternative way is to compare the different estimators directly. As an example, X-ray mass estimates generally differ sensibly from the strong/weak lensing estimates - however not always. The differences can be explained for different reasons depending on the cluster studied (*e.g.* Miralda & Babul 1995): *i)* projection effects: 2 clusters can be aligned on the line of sight and boost the lensing mass; *ii)* simple X-ray modeling: for example multiphase gas distribution are necessary in cooling flow clusters (*e.g* Allen, Fabian & Kneib 1996); *iii)* non-thermal effect can modify the central mass estimates; *iv)* the cluster just suffer a major merger event and the dynamical state of the gas can not be considered as in thermal equilibrium.

The canonical lensing clusters Abell 370 and Cl0024+1654 are two examples were the X-ray mass and lensing mass do not agree. For Abell 370, the disagreement is directly visible on the ROSAT/HRI X-ray surface brightness map that only peaks on the Southern cD galaxy, despite the lensing mass model requires a bimodal structure with equivalent mass around the 2 cDs – this difference, may however disappear when better X-ray observations (with *Chandra* and *XMM-Newton*) are made of this cluster. For Cl0024+1654, the X-ray emission is weak compared to the large Einstein ring observed. A recent redshift survey of ~300 cluster galaxies (Czoske et al. 2001) does however unveils some of the mystery. The redshift histogramme show a complex structure with a main relaxed structure compatible with the X-ray emission and a foreground structure along the line of sight that boost the lensing strength of this cluster.

Recently, Sunyaev-Zeldovich (SZ) effect has been routinely measured on the most X-ray luminous clusters (*e.g.* Carlstrom this conference). As SZ is probing the intra-cluster gas in a different way than X-ray observations, it is important to use SZ as a complementary approach to the lensing, X-ray and galaxies velocities estimators as a detailed study will teach us a lot on the cluster physics. Attempts of combining these different informations were presented during this Conference.

Ideally, one wants to looks at the mass properties of clusters as a function of time to derive their evolution. But to do that we need well defined samples of clusters, studied in an homogenous way. However, precise and systematic comparison is still relatively rare in the literature, as they usually rely on published data, either on the X-ray or on the lensing part, and thus do no tackle a well defined sample, nor do they address carefully the limits and bias of the two different approaches. This is however currently changing rapidly, as a number of dedicated surveys based on well defined cluster catalogue (Ebeling et al. 1996, 2000) are in progress (*e.g.* Czoske et al. this conference).

As an example of such developpements, we have started a thorough analysis of a sample of 12 $z \sim 0.2$ X-ray luminous clusters of galaxies selected from the XBACS catalogue (see Fig. 4). These clusters are followed up with the WFPC2 camera (*c.f.* Smith et al. 2000 for the first results) as well as the wide field CFHT12k camera on the lensing side. They will also all be look at with the $XMM - Newton$ telescope in order to relate the lensing and the X-ray mass reconstruction.

2.5 Dark lenses?

It has been known for a while that some of the multiple image quasars can only be modeled if an important external shear contribution was added to the main lens contribution (Keeton et al. 1997). In other cases the image separation between the multiple quasars is so large that large M/L for the main lensing galaxy are required. Thus, the existence of so-called *dark clusters* has been discussed. Recent deep inspection of these systems, followed by optical spectroscopy seems to reveal that *dark clusters* are not so dark after all (Benitez et al. 1999, Kneib et al. 2000, Soucail et al. 2000). A systematic deep survey of those multiple quasar systems where either a too high M/L ratio or a large external shear is required would be useful to understand whether *dark or not so dark* lump of matter are affecting the lensing of the quasars.

In this respect the detection of a dark lump of matter near the cluster Abell 1942 by Erben et al. (2000) is very puzzling. Either it is an extremely rare (?) cosmic conspiracy in the distribution of the faint galaxy ellipticities or what is detected is really a massive dark concentration of mass which true nature should be understood.

3 Cluster Lenses as Nature Telescopes

The most massive clusters can be used as efficient *Natural Telescope.* The key feature of these systems is that any distant object seen through the clusters is amplified (and distorted). This amplification can easily exceed a factor of > 2–$3\times$ for the central 4 sq. arcmin of the lens and will be still higher than $> 1.4\times$ over a 20 sq. arcmin field of view for the most massive clusters. The amplification provides a magnified view of a correspondingly smaller region of the source plane – so the 4 sq. arcmin region seen through the core of a cluster lens will actually translate to a < 2 sq. arcmin patch of the background sky. Thus a lens provides a more sensitive, but also more restricted, view of the high redshift sky. These effects, the amplification and the reduction in the available area, compensate each other for a source population with a count slope, $\alpha = 1$, where $N(> S) \propto S^{-\alpha}$ (or equivalently for a count slope $\gamma = 0.4$, where $N(m) \propto 10^{\gamma m}$). However,

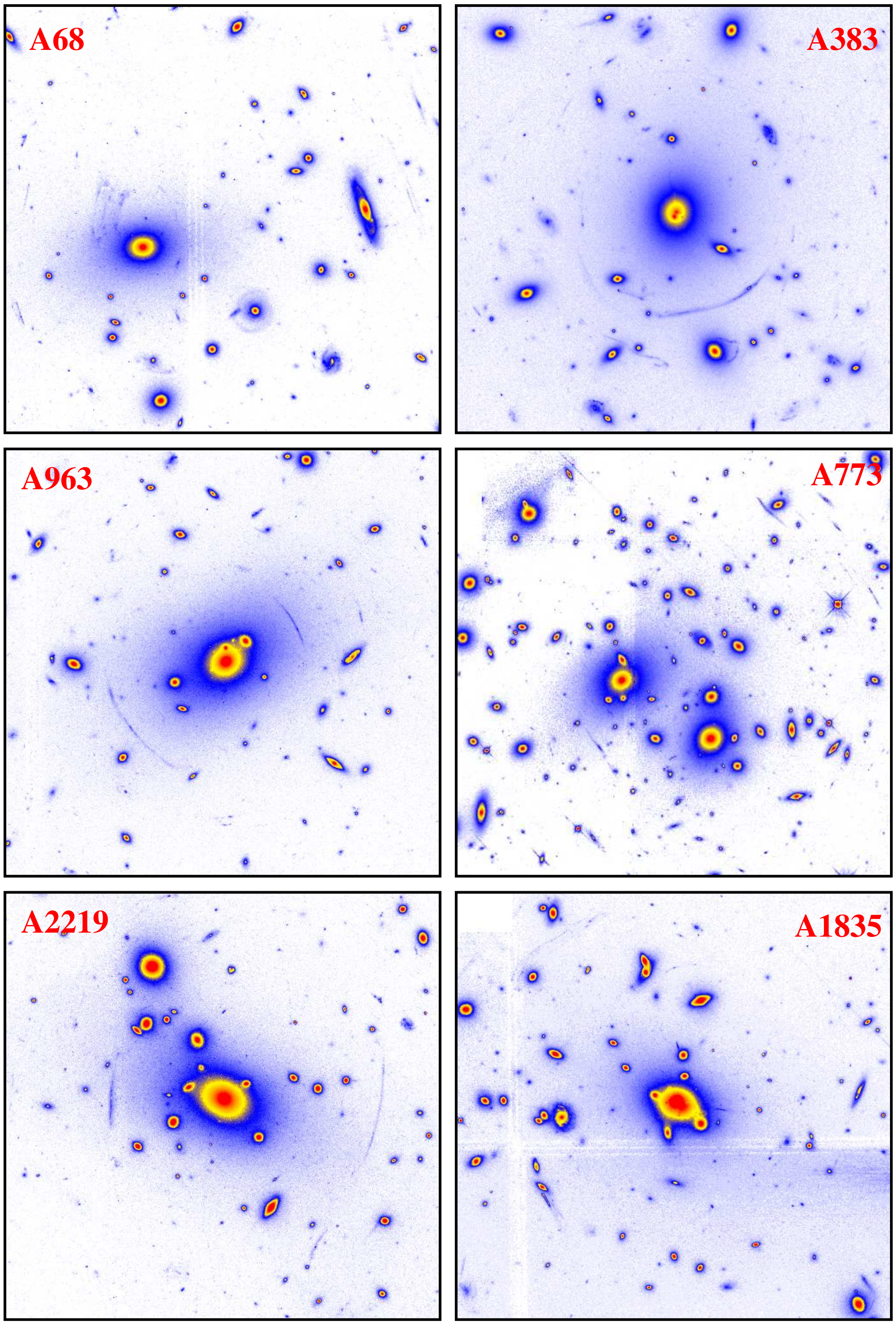

Figure 4: 6 of the 12 $z \sim 0.2$ X-ray luminous clusters of galaxies selected from the XBACS catalogue observed with the HST/WFPC2 camera. The field of view in 1 arcmin^2 except for Abell 773 which is 2.2 arcmin^2. Note the large number of strong lensing features.

the sources we identify in the lens field will be on average intrinsically $\sim 2\times$ fainter than those identified in an equivalent blank field.

Depending on the waveband used, we will either see, more, or less, sources than in blank field regions. As a first example, in the sub-mm waveband α is indeed very close to unity at the faintest flux (Smail et al. 1998, Blain et al. 1999) and so we expect to detect equivalent numbers of sources in lensed fields as in a blank field in the *same* exposure time. In the optical and Near-Infra red (NIR), the slope γ is about 0.3 at the faintest flux, thus we expect less sources than in blank field. Finally, in the Mid-Infra red (MIR), the slope α is ~ 1.5 at the faintest flux (Metcalfe et al. 1999, 2001) and we detect more sources than in the blank fields. A particular, the faintest MIR sources were detected in the deep ISOCAM pointing of Abell 2390 (Altieri et al. 1999).

The cluster-lens technique therefore allows you to reach below the sensitivity limit of normal observations. To successfully employ this lens technique we need to be able to correct the observations for the amplification by the cluster using a detailed mass model of the lens constructed from *HST* imaging is necessary (see section 2.1).

This technique has three major advantages: *i)* the image resolution in the source plane is effectively finer leading: to a fainter confusion limit for the sub-mm maps and MIR observations, and to smaller resolution elements in optical/NIR allowing to better identify the morphological aspects of these faint sources; *ii)* cluster-lenses are some of the best studied regions of the extragalactic sky – thus deep multi-wavelength observations are generally available making the identification of distant galaxy much easier; *iii)* in the case of rare events where the amplification is larger than 10, detailed physical observation of the distant lensed galaxy can be made on morphological aspects (Pelló et al. 1999, Soucail et al. 1999) or on spectroscopical aspects (Pettini et al. 2000).

Similar lensing techniques are starting to be used to search for high-redshift supernovae [SN] (*e.g.* Sullivan et al. 2000) or to detect Lyman-α emitters (Ellis et al. 2000, in prep). In the case of a detection of a SN in a multiple image, if we are able to measure a time delay, it will give a unique way to precisely constrain the *Hubble* parameter H_0.

4 Future and Prospects

Since the discovery of giant arcs in the late 80's gravitational lensing in cluster of galaxies has now become a powerful *cosmological* tool.

• We are now able to reconstruct the mass distribution in clusters in great details from the galaxy scale to the virial radius. The lensing mass estimate will be usefully compared to other mass estimators to provide critical information on the cluster physics (from the largest cluster scale to the galaxy scale) on well defined cluster samples.

• Wide field survey of *mass selected* cluster using lensing techniques will allow to make direct comparison to analytic/numerical models of the Universe and thus better understand the growth of structure and the large scale distribution of mass. It will also confirm or otherwise the existence of dark lump of mass, as well as how massive are the fillaments between galaxy clusters.

• Multiple images in cluster cores are about to measure directly the cosmological parameters through an optical geometrical test of the curvature of the Universe (see Golse et al. this conference), although more spectroscopic and mass modeling are needed, it is a very clean way to tackle this problem.

• Likewise, time dependant phenomenom like Supernovae or AGN fluctuations if observed behind well-known lensing clusters, may prove to be a very accurate way to probe the H_0, as it has been initiated using multiple quasars.

• Finally, massive clusters will always be the *unique place* to look at to boost telescope and instrument sensitivities at *all wavelength* to push ahead the discoveries to reach the faintest detection level and explore in details the morphology of distant galaxies.

Acknowledgments

I acknowledge support from the LENSNET network as well as from INSU/CNRS. I thanks all my collaborators for the fruitful work we are conducting to better understand our Universe using lensing *as a powerful tool. I specially thank D. Gerbal, F. Duret and the people organising this meeting in making it very lively and constructive.*

References

1. Allen, S., et al, 1996, *Mon. Not. Roy. Astr. Soc.* , 279, 615
2. Altieri, B., et al 1999, *Astron. Astroph.* , 343, L65
3. Bartelman, M., et al., 1996, *Astroph. Journ.* , 446, L115
4. Bezecourt, J., et al., 1999, *Astron. Astroph.* , 347, 21
5. Bezecourt, J., et al., 1999, *Astron. Astroph.* , 347, 21
6. Blain, A., et al 1999, *Astroph. Journ.* , 512, L87
7. Bridle, S., et al 1998, *Mon. Not. Roy. Astr. Soc.* 299, 895
8. Benitez, N., et al 1999, *Astroph. Journ.* , 527, 31
9. Carlstrom, J., et al 2000, *Physica Scripta*, volume T, 85, 148-155
10. Clowe, D., et al 2000, *Astroph. Journ.* , 539, 540
11. Czoske, O., et al 2001, *Astron. Astroph.* in preparation.
12. Ebeling, H., et al 1996, *Mon. Not. Roy. Astr. Soc.* 281, 799
13. Ebeling, H., et al 2000, *Astroph. Journ.* submitted (astro-ph/0009101)
14. Ebbels, T., et al 1998, *Mon. Not. Roy. Astr. Soc.* , 295, 75
15. Erben, T., et al 2000, *Astron. Astroph.* , 355, 23
16. Fort, B., et al 1992, *Astroph. Journ.* , 399, L125
17. Hoekstra, H., et al 2000, *Astroph. Journ.* , 532, 88
18. Geiger, B., Schneider, P., 1998, *Mon. Not. Roy. Astr. Soc.* , 295, 497
19. Geiger, B., Schneider, P., 1999, *Mon. Not. Roy. Astr. Soc.* , 302, 118
20. Joffre, M., et al 2000 *Astroph. Journ.* , 534, L131
21. Kaiser, N., & Squires, G., 1993 *Astroph. Journ.* , 404, 441
22. Kaiser, N., 1995 *Astroph. Journ.* , 439, L1
23. Kaiser, N., et al 1995 *Astroph. Journ.* , 449, 460
24. Kaiser, N., et al 2000 *Astroph. Journ.* , submitted (astro-ph/9809268)
25. Kaiser, N., 2000 *Astroph. Journ.* , 537, 555
26. Keeton, C. et al, 1997 *Astroph. Journ.* , 482, 604
27. Kneib, J.–P. et al, 1993, *Astron. Astroph.* , 273, 367
28. Kneib, J.–P. et al, 1994a, *Astron. Astroph.* , 290, L25
29. Kneib, J.–P. et al, 1994b, *Astron. Astroph.* , 286, 701
30. Kneib, J.–P. et al, 1996, *Astroph. Journ.* , 471, 643
31. Kneib, J.–P. et al, 2000 *Astroph. Journ.* , 544, L35 (astro-ph/0006106)
32. Kochanek, C. et al, 1995 *Astroph. Journ.* , 445, 549
33. Kassiola, A. et al, 1992 *Astroph. Journ.* , 400, 41
34. Kuijken, K., 1999 *Astron. Astroph.* , 352, 355
35. Lewis, J., Smail, I. & Couch, W., 2000, *Astroph. Journ.* 528, 118
36. Lombardi, M. & Bertin, G., 1998, *Astron. Astroph.* 348, L38
37. Mellier, Y., et al, 1993, *Astroph. Journ.* , 407, 33
38. Metcalfe, L. et al, 1999 In "The Universe as seen by ISO", 1999, eds.: P.Cox, M.F.Kessler, ESA Publication Division, ESTEC, Noordwijk, NL

39. Miralda-Escudé, J., & Babul, A., 1995, *Astroph. Journ.* , 449, 18
40. Natarajan, P., Kneib, J.–P. 1996, *Mon. Not. Roy. Astr. Soc.* , 283, 1021
41. Natarajan, P., Kneib, J.–P. 1997, *Mon. Not. Roy. Astr. Soc.* 287, 833
42. Natarajan, P., et al, 1998, *Astroph. Journ.* , 499, 600
43. Natarajan, P., et al, 2001, *Astroph. Journ.* , in preparation
44. Pelló, R., et al, 1999, *Astron. Astroph.* , 346, 359
45. Pettini, M., et al, 2000, *Astroph. Journ.* , 528, 96
46. Rix, H.W., et al 1997, *Astroph. Journ.* , 448, 702
47. Rhodes, J., et al 2000, *Astroph. Journ.* , 536, 79
48. Schneider, P., et al, 1992, "Gravitational Lensing' A&A library series.
49. Schneider, P., 1995, *Mon. Not. Roy. Astr. Soc.* , 302, 639
50. Seitz, C., & Schneider, P., 1995, *Astron. Astroph.* , 297, 287
51. Seitz, S., & Schneider, P., 1996, *Astron. Astroph.* , 305, 383
52. Smail, I., et al 1998, *Astroph. Journ.* , 507, L21
53. Smith, G., et al 2000, *Astroph. Journ.* , in press, (astro-ph/0008315)
54. Sullivan, M., et al 2000, *Mon. Not. Roy. Astr. Soc.* , 319, 549 228)
55. Soucail, G., et al 2000, *Astron. Astroph.* , in press, (astro-ph/0006382)
56. van Albada, T.S., et al, 1985, *Astroph. Journ.* , 295, 305